JOURNAL OF MATERIALS SCIENCE 32 (1997) 3891–3903

Mechanical properties and microstructural stability of wrought, laser, and electron beam glazed NARloy-Z alloy at elevated temperatures

J. SINGH
Applied Research Laboratory, The Pennsylvania State University, University Park, PA 16804, USA

G. JERMAN, R. POORMAN, B. N. BHAT
NASA-Marshall Space Flight Center, Huntsville, AL 35812, USA

A. K. KURUVILLA
IIT Research Institute, NASA-Marshall Space Flight Center, Huntsville, AL 35812, USA

Microstructure of wrought, laser and electron beam processed NARloy-Z (Cu-3 wt % Ag–0.5 wt% Zr) was investigated for thermal stability at elevated temperatures 539–760 °C (1100 to 1400°F) up to 94 h. Optical and scanning electron microscopy and electron probe microanalysis were employed for studying microstructural evolution and kinetics of precipitation. Grain boundary precipitation and precipitate free zones (PFZs) were observed in the wrought alloy after exposing to temperatures above 605 °C (1120 °F). Fine-grained microstructure observed in the laser and electron beam (EB) processed NARloy-Z was much more stable at elevated temperatures. Tensile properties of laser and EB glazed NARloy-Z can be tailored by giving suitable heat treatments and maintaining the same strength with increased ductility. Microstructural changes correlated well with hardness measurements and mechanical properties.

1. Introduction

Continuous efforts are under way to develop an alloy which can have an exceptional high temperature strength and good thermal conductivity for high heat flux applications such as regeneratively cooled rocket motors, combustion chambers and heat exchangers. A series of copper based alloys was developed by the addition of alloying elements such as Cr, Co, Ag, Zr, Nb, etc., in various combinations at different laboratories. The NARloy-Z™ (Cu–3 wt % Ag–0.5 wt % Zr + traces of O_2, $\sim$50 p.p.m), which is a trade mark of Rocketdyne (division of Rockwell International), is commonly used for the above mentioned applications. NARloy-Z is used in both wrought and cast forms for fabricating engine components.

Wrought NARloy-Z is used in the NASAs Space Shuttle Main Engine (SSME)–Main Combustion Chamber (MCC) as well as rocket engines. Hot wall or liner is the most critical section of the SSME–MCC. Since the NARloy-Z™ alloy is proprietary to Rocketdyne, very limited information is available in the literature. Therefore, an effort was directed to evaluate the microstructure of NARloy-Z at elevated temperatures and correlate it with the mechanical properties.

2. Background

NARloy-Z is a ternary alloy (Cu–3 wt % Ag–0.5 wt % Zr) derived from the binary alloy NARloy-A (Cu–3 wt % Ag). Therefore, an understanding of the physical metallurgy of NARloy-A is necessary to understand NARloy-Z, especially the role of the Zr addition.

2.1. NARloy-A

NARloy-A undergoes quite complex decomposition reactions. Ag-rich phases experience continuous/discontinuous precipitation during ageing at 480 °C (900 °F) for 4 h. Continuous precipitation can take place before, during, or after discontinuous precipitation [1].

Continuous precipitation is responsible for age hardening of the alloy and it occurs when an Ag-rich phase is uniformly distributed into the matrix. These precipitates have the same orientation as the matrix, but a slightly different lattice parameter, making them semi-coherent.

Discontinuous precipitation refers to selective grain boundary precipitation. This condition results in a eutectic-like structure that reduces the mechanical properties of NARloy-A.

0022–2461

2.2. NARloy-Z and the Zr addition

Reports indicate that discontinuous precipitation is inhibited when Zr is added to Cu–3 wt % Ag. The presence of Zr makes three major contributions to the microstructure of NARloy-Z [2]:

1. Grain growth is restricted by pinning Cu grain boundaries with Cu–Ag–Zr intermetallic compounds.
2. Discontinuous precipitation is inhibited by Zr, which promotes homogeneous precipitation of Ag-rich phases on ageing.
3. Zr deoxidizes the alloy and removes Cu_2O from the grain boundaries, improving ductility at elevated temperatures.

Based on the binary phase diagrams, the maximum solid solubility of Zr in the Cu matrix is about 0.1 wt % at 935 °C (1715 °F). Since NARloy-Z only contains about 0.5 wt % Zr, the excess will precipitate either as a Zr-rich intermetallic phase or as zirconium oxide (Zr_2O_3).

To achieve the best thermal conductivity and high temperature mechanical properties, the recommended heat treatment cycle for wrought NARloy-Z is to solutionize at 935 °C (1715 °F) for 4 h, water quench, and then age at 480 °C (900 °F) for 4 h. The Ag-rich phase will uniformly precipitate out, giving an age hardening effect.

Wrought NARloy-Z contains traces of O_2 ($\sim$ 50 p. p.m.). Zr is assumed to absorb any O_2 present in the matrix, forming stable zirconium oxide which is uniformly dispersed throughout the matrix. The Ag-rich phase is assumed to provide precipitation hardening during the heat treatments discussed above. However, the formation of complex Zr- and Ag-rich intermetallic phases and their influence on the microstructure and mechanical properties are not well understood.

Three different approaches can be taken to increase the service life of the MCC liner. One approach is to develop a new liner alloy with higher thermal stability, better mechanical properties and improved thermal conductivity [3]. A second approach is to apply thermal barrier coatings such as NiCrAlY, TiN, etc., to the liner to lower the operating temperatures. The third approach is to improve the microstructure and thermal stability of the wrought NARloy-Z liner by surface glazing. This paper presents the third approach which is a relatively new technique in which the surface is rapidly melted and resolidified with a high energy laser or electron beam. The glazed area develops a fine-grained microstructure with uniform distribution of second phases in the matrix that is much more stable at elevated temperatures.

3. Experimental procedure

Wrought NARloy-Z was selected as a starting material for laser and electron beam (EB) glazing. The samples of wrought NARloy-Z were solutionized at 935 °C (1715 °F) before studying the precipitation kinetics. Specimens of wrought, laser and electron beam glazed NARloy-Z were exposed to elevated temperatures ranging from 593 to 760 °C (1100 to 1400 °F) for up to 84 h in a drop-through vacuum furnace to effect microstructural changes and then rapidly quenched with helium gas. Metallographic samples were then prepared and etched with an ammonium persulphate solution [$(NH_4)_2S_2O_8$ per 100 ml H_2O]. Vickers hardness measurements were made with a 200 g weight for the purpose of comparison of microstructure with hardness. The samples were examined with an optical microscope, a Hitachi S-4000 field emission scanning electron microscope (SEM), and a Cameca SX-50 electron microprobe. Elemental analyses of different phases were performed using qualitative energy dispersive spectroscopy (EDS) and electron probe microanalysis (EPMA).

Tensile tests were conducted using flat specimens to determine the effect of glazing on strength and ductility of NARloy-Z. The strain rate of testing was $8.3 \times 10^{-4}\,s^{-1}$. All tests were performed at 538 °C (maximum design operating temperature) in a helium environment. The heating rate for these elevated temperature tests was 0.6 °C s^{-1} and specimens were held at temperature for about 2 h prior to testing. Fractography of the tensile tested samples was done in the SEM.

4. Results and discussion

4.1. Hardness

Hardness change in wrought and laser-glazed NARloy-Z as a function of exposure time up to 84 h at 593 °C (1100 °F) is shown in Fig. 1 and at 649 °C (1200 °F) in Fig. 2. There was some drop in the hardness of the laser glazed NARloy-Z as compared to the wrought alloy after exposing at 593 °C (1100 °F) for up to 84 h. At 649 °C (1200 °F), hardness values remained constant for up to 24 h and then dropped slowly by $\sim$ 7% as a function of time (Fig. 2). Fig. 3 shows hardness changes as a function of temperature from 593 to 760 °C (1100 to 1400 °F) for a constant exposure time (24 h).

The hardness of EB-processed NARloy-Z was measured before and after exposure at 705 °C (1300 °F) for 24 h. The hardness values were similar to the laser-glazed alloy. Andrus and Bourdeau [3] also obtained comparable values when they measured the hardness of wrought and EB-processed NARloy-Z.

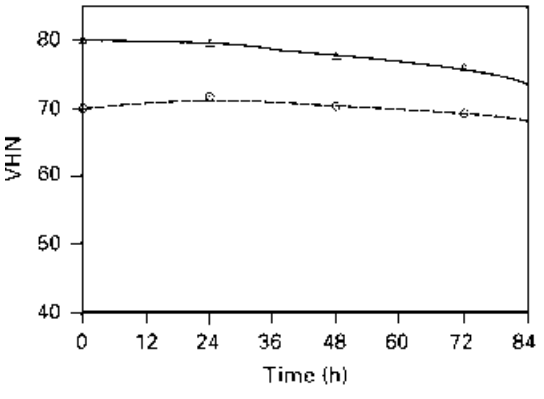

Figure 1 Hardness change in wrought (○) and laser-glazed (△) NARloy-Z as a function of time at 593 °C (1100°F).

The average hardness of laser-glazed NARloy-Z was approximately 15% higher than the wrought alloy and remained so even after exposing to elevated temperatures ranging from 593 to 760 °C (1100 to 1400 °F) as shown in Figs 1 to 3. Increased hardness was probably due to the fine-grained microstructure and uniform distribution of the second phase in the Cu matrix. This subject will be discussed further in the next section.

4.2. Mechanical properties

The effect of processing on the tensile properties of NARloy-Z is presented in Table I. Laser glazing doubles the yield strength of wrought NARloy-Z at 538 °C, from 76 MPa in the wrought condition to 152 MPa in the laser-glazed condition. Although not to the same extent, there is a significant increase in the UTS, from 117 to 165 MPa, associated with the glazing. The increase in strength is accompanied by a reduction in ductility, elongation decreasing from 60 to 38%. Clearly, the increase in strength can be attributed to the extent of solid solubility of Zr in the alloy matrix and residual stresses associated with solidification. The laser-glazed alloy was subsequently heat treated for improved ductility. The effect of heat treatment on strength and ductility is also presented in Table I. The 704 °C/2 h treatment resulted in a decrease in strength and a considerable increase in the ductility. The resultant (post-heat treatment) ductility of the laser glazed specimen (58%) approaches that of the wrought specimen (60%). Even though this heat treatment results in decreased strength, the yield strength of the laser glazed specimen is 14 MPa (18%) higher than the wrought specimen. Heat treatment of the laser glazed specimen at 760 °C for 2 h resulted in strength levels similar to that of the wrought alloy. However, the ductility of this specimen was 80% compared to the wrought alloy that displayed 60%. It is apparent that laser glazing of the wrought NARloy-Z can enhance ductility by as much as 33%, maintaining equivalent levels of strength. From the microstructural standpoint, glazing extends the solid solubility of Zr and Ag and enhances the precipitation of free Ag in contrast to Ag- and Zr-rich intermetallic in the wrought alloy. The absence of intermetallic at grain boundaries in the glazed alloy is most likely the reason for its higher ductility at elevated temperature. This also is indicative of the wide variety of strength–ductility combinations that can be achieved in this alloy with laser glazing. Therefore, it is possible to tailor this alloy for specific liner applications from the standpoint of tensile properties. The high levels of ductility suggest that laser glazing could improve the low cycle fatigue (LCF) resistance of wrought NARloy-Z. This is an added advantage because LCF caused by thermal cycling is a concern in these applications.

Electron beam and tungsten inert gas (TIG) glazing produced identical strength and ductility results as shown in Table I. Heat treating the glazed alloy at lower temperature (649 °C) for longer periods of time (48 h) resulted in acceptable strength values but

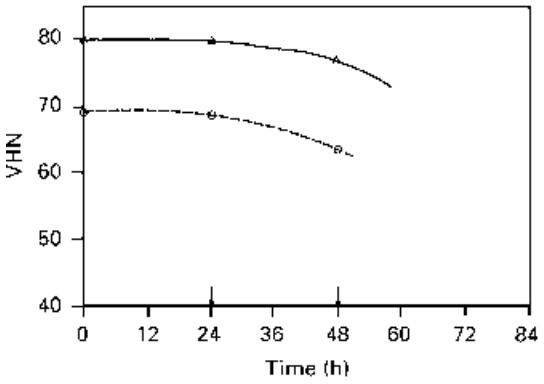

Figure 2 Hardness change in wrought (○) and laser-glazed (△) NARloy-Z as a function of time at 649 °C (1200 °F).

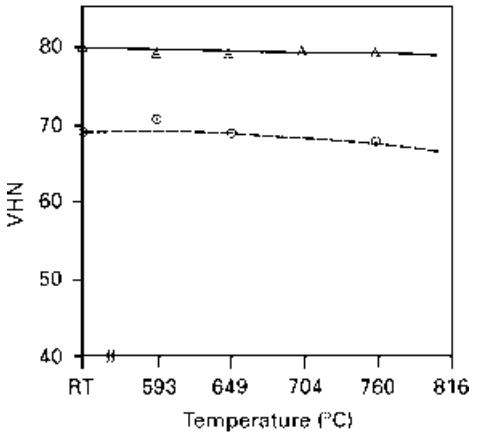

Figure 3 Hardness change in wrought (○) and laser-glazed (△) NARloy-Z as a function of temperatures ranging from 593 to 760 °C (1100 to 1400 °F) for 24 h.

TABLE I Mechanical properties of NARloy-Z

Condition	Heat treatment	Test temperature (°C)	YS (MPa)	UTS (MPa)	Elongation (%)
Wrought	941 °C (1725°F) for 1 h/Q	75	96.5	303.4	55
(baseline)	482 °C (900°F) for 4 h/Q	538	75.8	117.2	60
Laser glazed	None/as-glazed	538	144.8	165.5	44
EB glazed	482 °C (900°F) for 4 h/Q	538	110.3	124.1	16
EB glazed	649 °C (1200°F) for 48 h/Q	538	75.8	103.4	51
EB glazed	704 °C (1300°F) for 2 h/Q	538	89.6	117.2	57
Laser glazed	704 °C (1300°F) for 2 h/Q	538	89.6	117.2	52
EB glazed	760 °C (1400°F) for 2 h/Q	538	62.1	117.2	69
Laser glazed	760 °C (1400°F) for 2 h/Q	538	75.8	110.3	80
TIG glazed	649 °C (1200°F) for 48 h/Q	538	89.6	110.3	49

ductilities were always significantly higher when the alloy was heat treated at higher temperatures for shorter periods of time. Given that the operating temperatures are close to 538 °C, the elevated temperature heat treatment will ensure microstructural stability during operation in addition to producing superior ductility.

4.3. Microstructural evolution

4.3.1. Wrought NARloy-Z

In general, the wrought NARloy-Z starting material had a coarse-grained microstructure (Fig. 4a) with an uneven distribution of secondary precipitates. Microprobe analyses showed that Zr was present (as zirconium oxide, probably Zr_2O_3, Fig. 4b). Ag- and Zr-rich intermetallic phases were present in the Cu matrix (Fig. 4c to d). In addition, oxides of Ag and Cu were present in the matrix. The secondary phases varied in size from 1 to 10 μm. The average grain size was approximately 150 μm. Fig. 5 shows precipitation and coarsening in the Cu matrix and at the grain boundaries after exposure to 593 °C (1100°F) for up to 94 h. Fig. 6 shows the microstructural changes in NARloy-Z after exposure to 649 °C (1200°F) up to 48 h. Precipitate-free zones (PFZs) were observed near the grain boundaries and large intermetallic phases as shown by arrows in Fig. 6. The size of precipitates and PFZ width increased at 649 °C (1200°F) as exposure time increased from 24 to 48 h. After 24 h exposure at 649 °C (1200°F), the volume fraction and size of precipitates in the Cu matrix (Fig. 6b) were noticeably larger than those in the starting material. The same was true for NARloy-Z exposed to 593 °C (1100°F) for ~94 h (Fig. 5).

After 24 h exposure at 705 °C (1300°F), the wrought NARloy-Z showed relatively large intermetallic precipitates in the Cu matrix and grain boundaries (Fig. 7). The PFZ width was also larger than that exposed to 1200°F for 48 h (compare Figs 6 and 7). EDS analysis was used to identify the matrix and grain boundary precipitates as Ag- and Zr-rich intermetallic phases (Fig. 8), and an EPMA was carried out across the grain boundary (line AB as shown in Fig. 7a) to confirm the analysis. No concentration gradient of Zr and Ag solute atoms was observed across the PFZ and grain boundary (Fig. 9), indicating that the precipitation reaction was essentially complete.

After exposure at 760 °C (1400°F) up to 48 h, the wrought NARloy-Z showed even coarser precipitation of intermetallic phases (Fig. 10). The PFZ width was also larger than the NARloy-Z exposed to 649 to 705 °C (1200 to 1300°F).

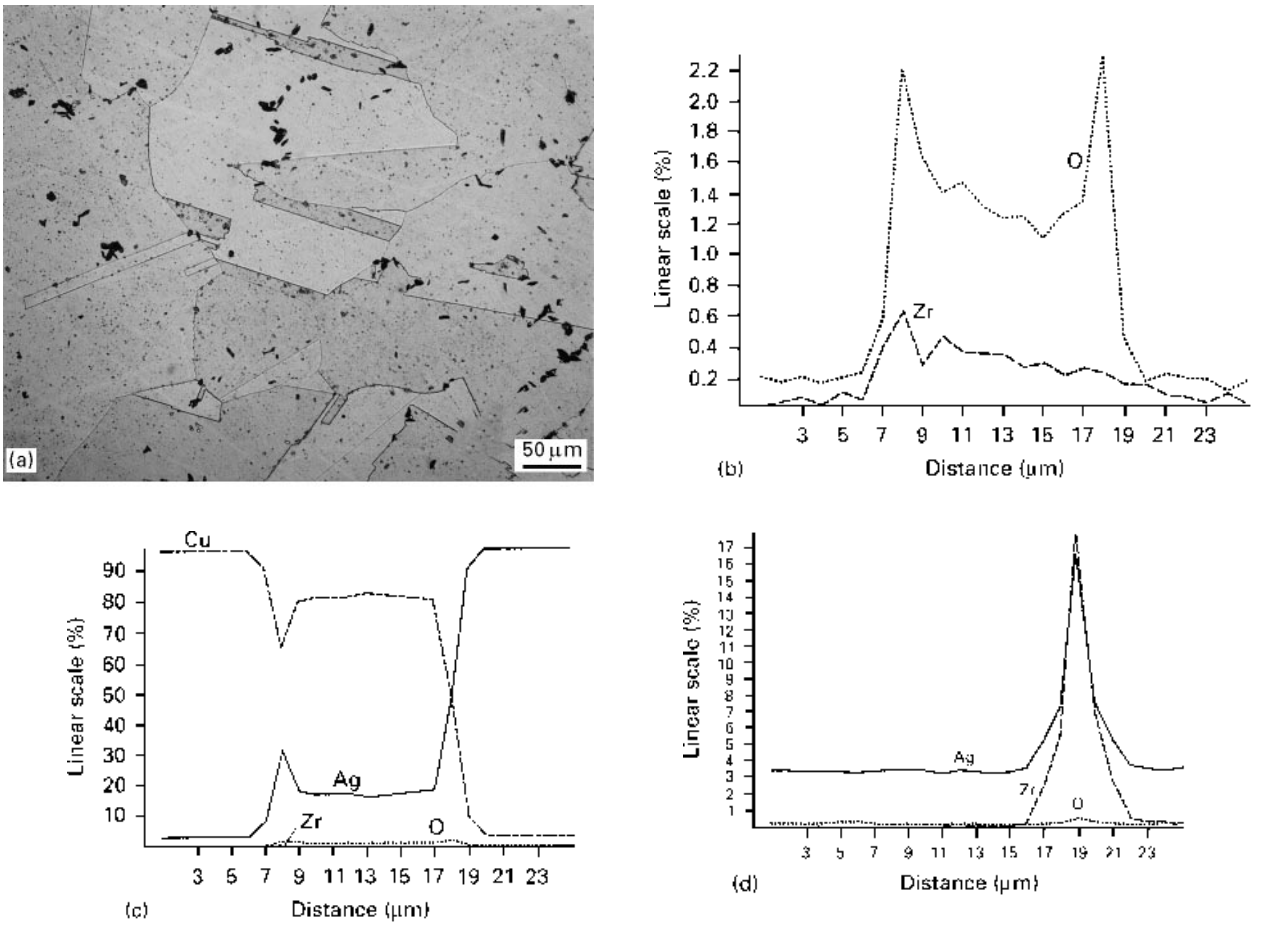

Figure 4 (a) Wrought NARloy-Z showing two-phase microstructure (intermetallic CuAgZr and zirconium oxide) in Cu matrix. (b) EPMA across the second phase in wrought NARloy-Z, showing Zr present as Zr_2O_3 into Cu matrix. (c) EPMA across the second phase in wrought NARloy-Z, showing Ag-rich intermetallic phases present into Cu matrix. (d) EPMA across the second phase in wrought NARloy-Z, showing Zr-rich intermetallic phases present into Cu matrix.

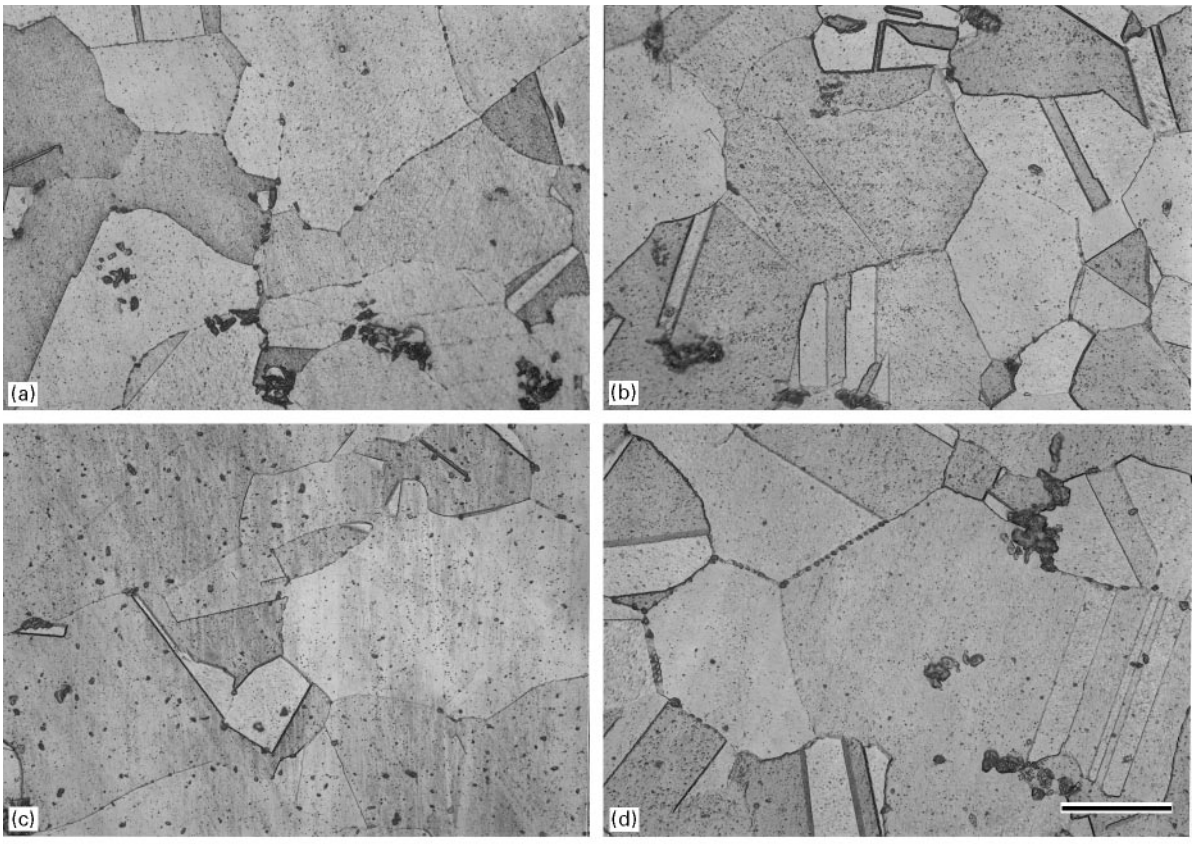

Figure 5 Wrought NARloy-Z showing precipitation of second phases (intermetallic CuAgZr and zirconium oxide) in Cu matrix after exposure at 593 °C (1100 °F) for (a) 24, (b) 48, (c) 72, and (d) 94 h.

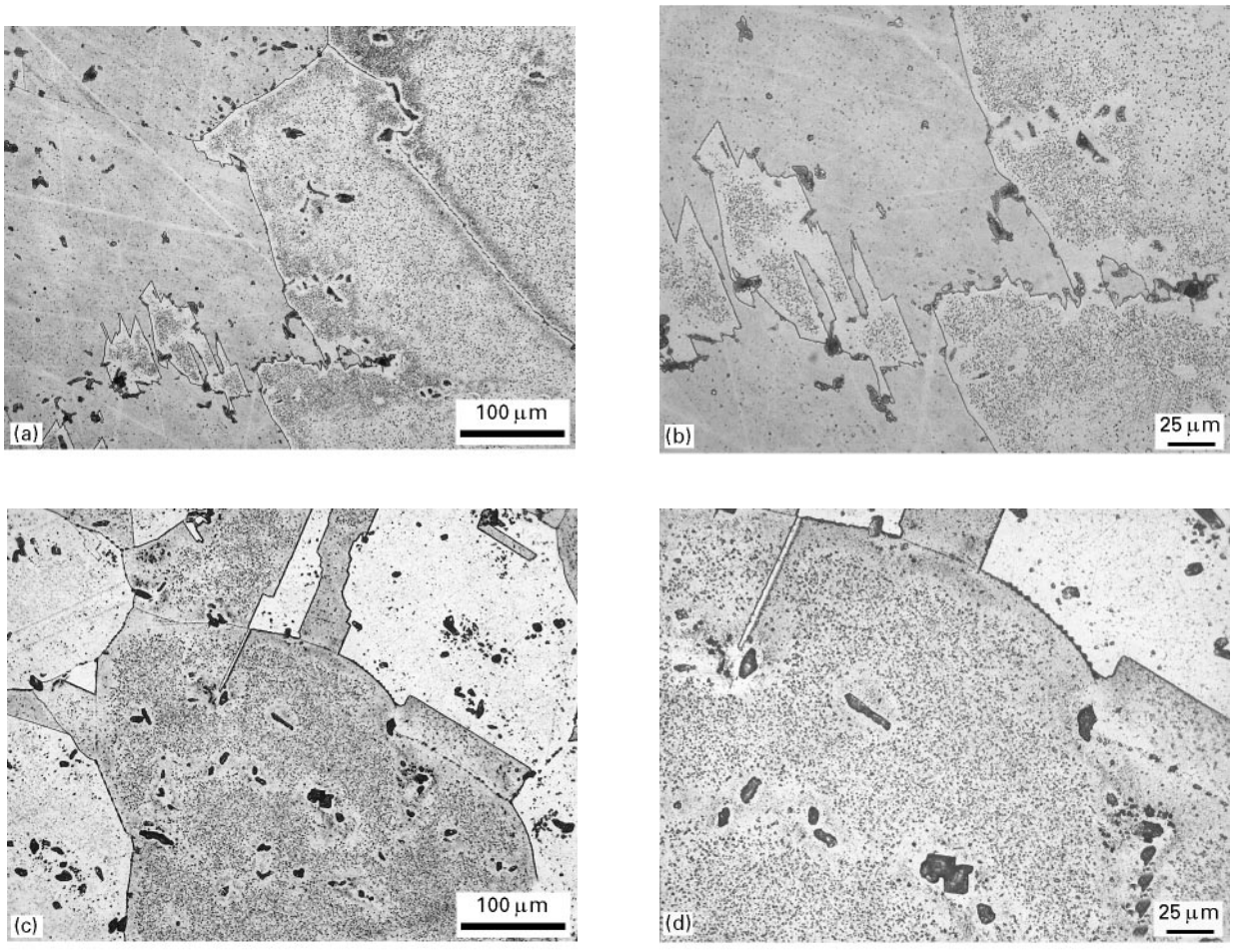

Figure 6 Wrought NARloy-Z showing grain boundary precipitation, PFZ near grain boundaries, and precipitation of second phases (intermetallic CuAgZr and zirconium oxide) in Cu matrix after exposure at 649 °C (1200 °F) for (a) and (b) 24 h and (c) and (d) 48 h.

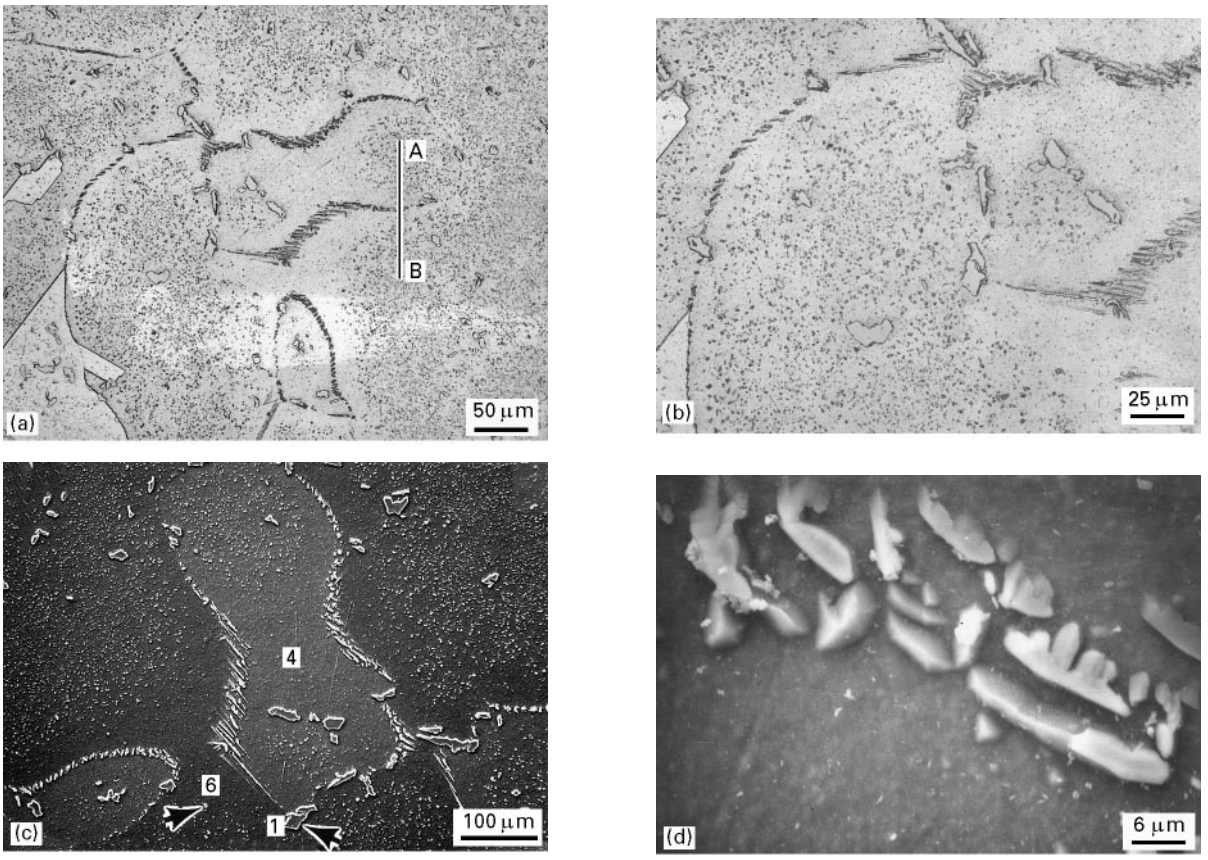

Figure 7 Optical ((a) low magnification and (b) high magnification) and SEMC (c) low magnification and (d) high magnification) micrographs of the wrought NARloy-Z showing grain boundary precipitation, PFZ near grain boundaries, and second phase precipitation (intermetallic CuAgZr and zirconium oxide) in Cu matrix after exposure at 705 °C (1300 °F) for 24 h.

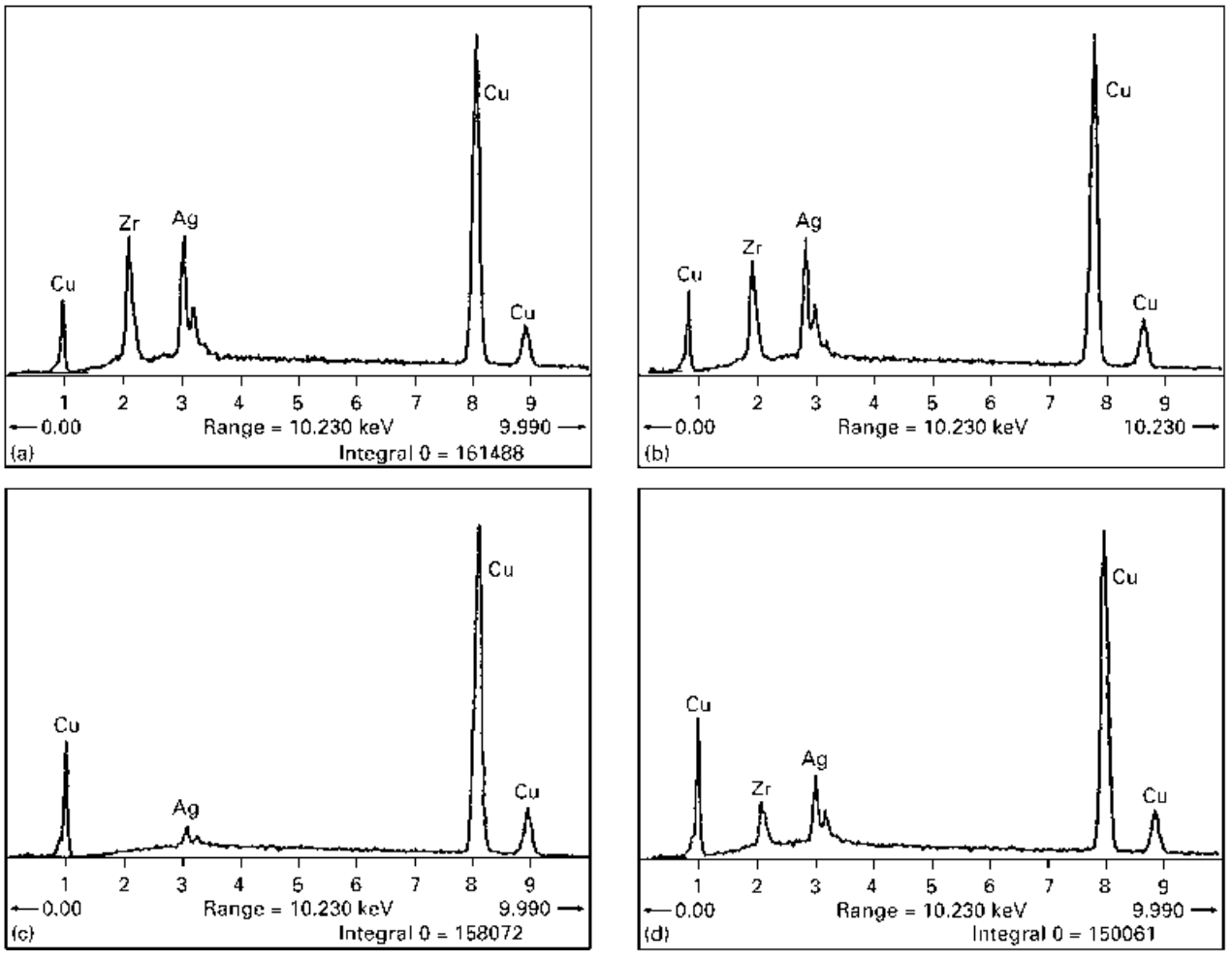

Figure 8 EDS spectrum from precipitates (regions 1(a) and 2(b)) and matrix (regions 4(c) and 6(d)), as marked in Fig. 7c.

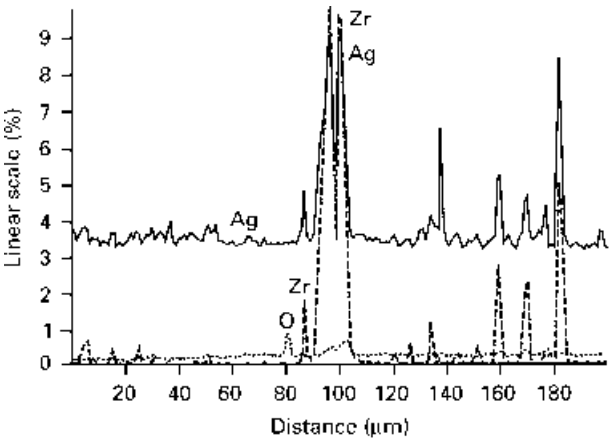

Figure 9 EPMA across precipitate, as marked in Fig. 7a.

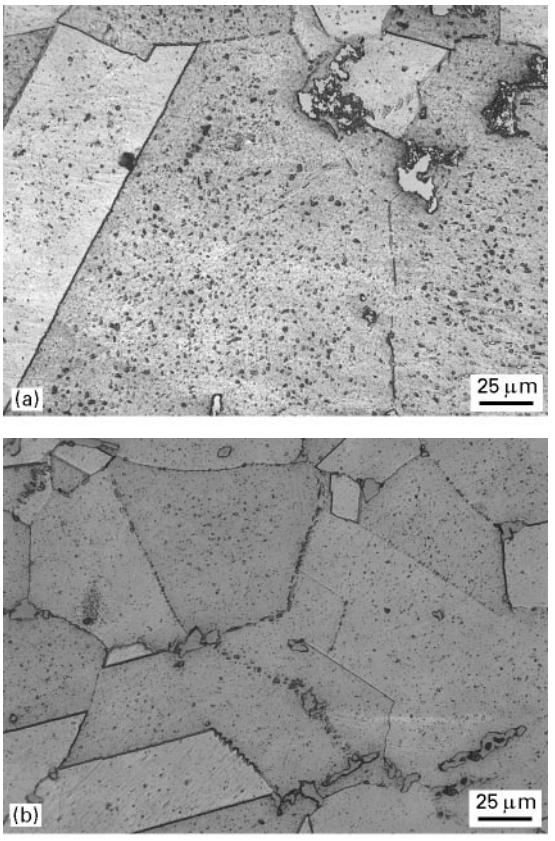

Figure 10 Wrought NARloy-Z showing grain boundary precipitation, PFZ near grain boundaries, and second phase precipitation (intermetallic CuAgZr and Zr oxide) in Cu matrix after exposure at 760 °C (1400°F) for (a) 24 and (b) 48 h.

Two significant features are noteworthy in the wrought NARloy-Z exposed from 593 to 760 °C (1100 to 1400°F): (a) precipitation and coarsening of Ag- and Zr-rich intermetallic phases in the matrix and at grain boundaries and (b) PFZs near large intermetallic phases and at grain boundaries (Figs 6 to 10).

At temperatures above 649 °C (1200°F), PFZ formation probably occurred in response to grain boundary precipitation, migration and long range solute atom diffusion. The PFZ width increased as a function of temperature (Fig. 11). Extrapolation of the PFZ size to zero in Fig. 11 indicates that PFZ occurs only above 605 °C (1120°F). The prior investigation [6] was conducted below 538 °C (1000°F), which may be why the investigators did not report PFZ formation in wrought NARloy-Z.

When microstructure and hardness measurements were compared, good correlation was obtained between the two. Hardness decreased as the exposure temperatures increased from 649 to 760 °C (1200 to 1400°F), probably due to rapid depletion of Ag and Zr solute atoms from the matrix and coarsening of intermetallic phases in the Cu matrix (Figs 1 to 3).

4.3.2. Laser and electron beam (EB) glazed NARloy-Z

Metallographic examination of laser-glazed NARloy-Z revealed uniform distribution of second phases in the Cu matrix (Fig. 12). No grain boundary segregation was observed. In the rapidly solidified region, the average grain size was 100 μm which is about half the wrought NARloy-Z grain size (150 to 300 μm). No significant change in the microstructure was observed on exposure at 593 °C (1100°F) for up to 84 h (Fig. 13). A small amount of coarsening of the second phase was observed as a function of time. Further coarsening of

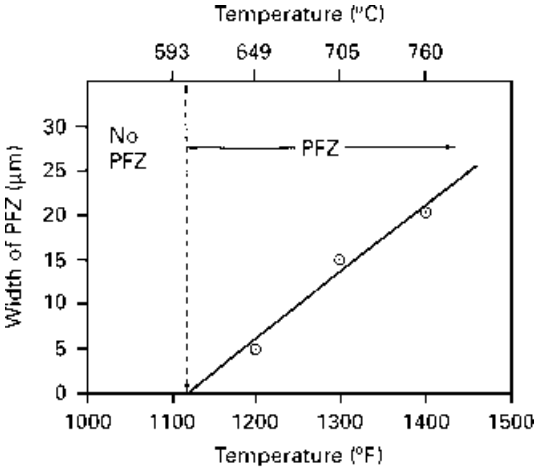

Figure 11 Plot of PFZ width as a function of exposure to temperatures ranging from 649 to 760 °C (1200 to 1400 °F).

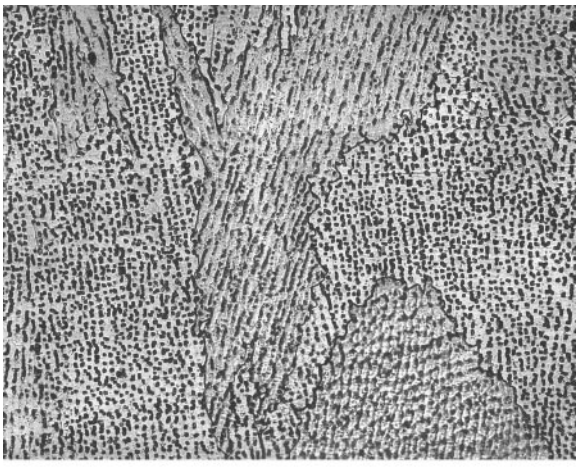

Figure 12 Laser-glazed NARloy-Z showing uniform distribution of second phases in Cu matrix.

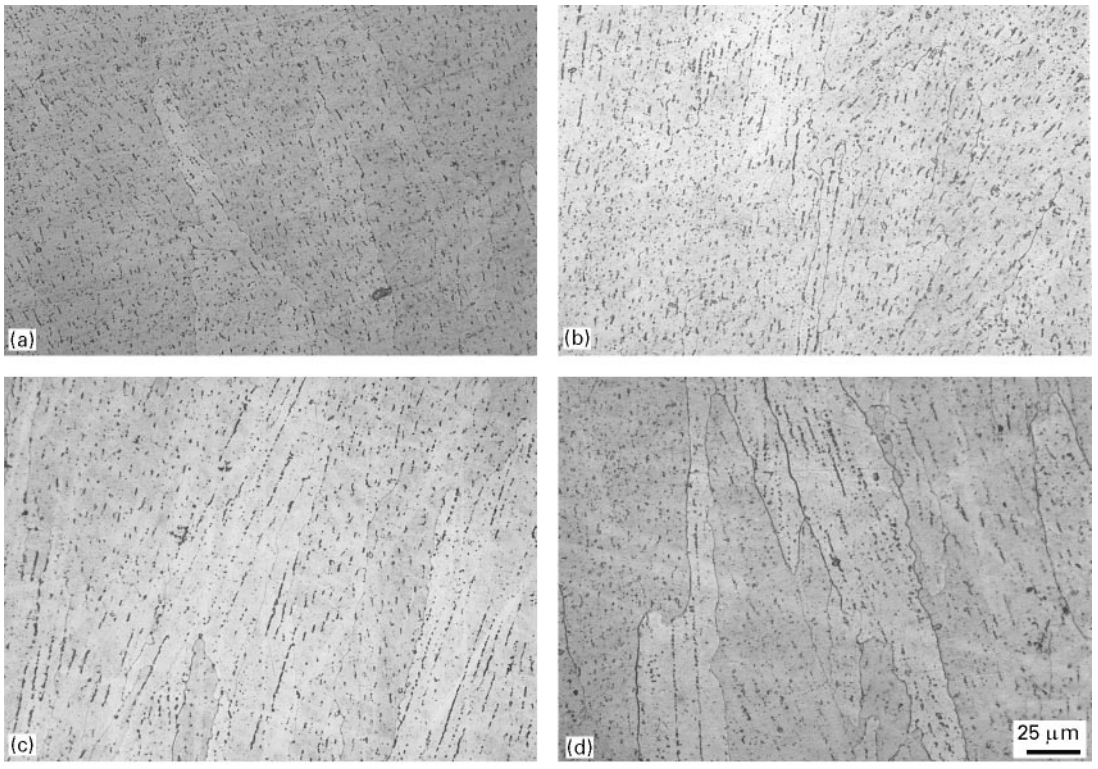

Figure 13 Laser-glazed NARloy-Z showing uniform distribution of second phases in Cu matrix after exposure at 593 °C (1100 °F) for (a) 24 h, (b) 48 h, (c) 72 h, and (d) 96 h.

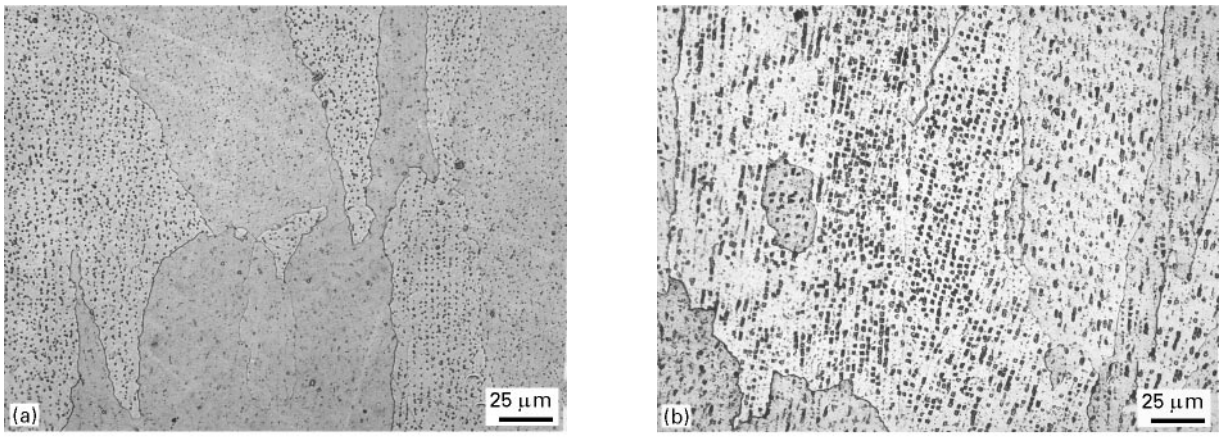

Figure 14 Laser-glazed NARloy-Z showing uniform distribution of faceted second phases in Cu matrix after exposure at 649 °C (1200 °F) for (a) 24 and (b) 48 h.

second phases was observed after exposing at 649 °C (1200°F) for up to 48 h (Fig. 14a and b). These precipitates were aligned and had a faceted morphology (Fig. 14b). However, the second phase sizes were still small and averaged less than 0.5 μm, smaller than those observed in wrought NARloy-Z (10 μm, see Fig. 4).

EPMA technique was used to determine the concentration profile across the aligned precipitate (Figs 14 and 15). Faceted precipitates were mostly Ag, whereas most of the Zr was found in the matrix (Fig. 15). The second phases coarsened further on exposure to higher temperatures 705 to 760 °C (1300 to 1400°F), but the average size was still small and remained at less than 0.5 μm (Figs 16 and 18). Unlike the wrought NARloy-Z, grain boundary precipitation and PFZs were not observed in the Cu matrix in any of the experiments.

Electron beam glazed NARloy-Z showed a fine-grained microstructure (Fig. 19), comparable to laser-glazed NARloy-Z (Fig. 12). The melt pool ranged in depth from 0.6 to 2 mm (25 to 80 mils), depending upon processing conditions such as traverse speed and beam current (Fig. 20).

Faceted and aligned precipitates were observed in the Cu matrix of samples exposed to 704 to 760 °C (1300 to 1400°F) for up to 48 h (Fig. 21). The second phase averaged less than 0.5 μm in size. No significant differences were seen in the microstructure of EB-processed and laser-glazed samples exposed to temperatures from 649 to 769 °C (1200 to 1400°F).

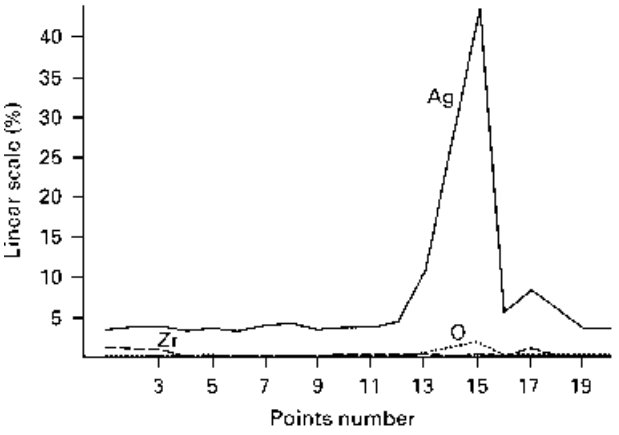

Figure 15 EPMA across the faceted precipitate, seen in Fig. 14.

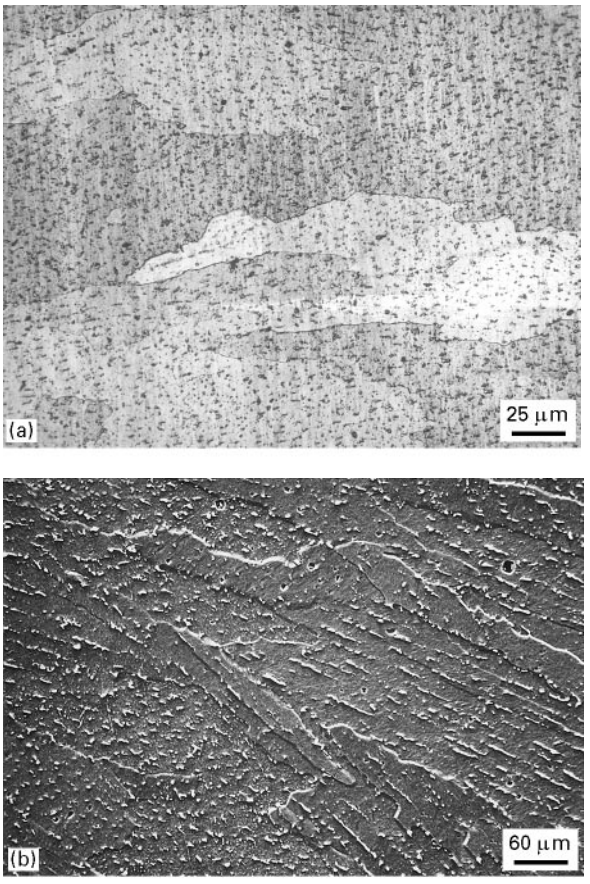

Figure 16 Laser-glazed NARloy-Z showing uniform distribution of second phases in Cu matrix after 24 h at 649 °C (1200 °F).

Laser-glazed NARloy-Z was always harder than the wrought alloy by 15 % or more (Fig. 1). The higher hardness of the laser-glazed alloy was probably due to the small-grained microstructure, fine and uniform distribution of second phase in the Cu matrix and absence of PFZ and/or grain boundary precipitations. Its overall microstructure remained the same even after exposure to high temperature, with the exception of slight coarsening of the second phase. The wrought alloy on the other hand consisted of a microstructure that was significantly changed by exposure to high temperatures (Figs 6 to 10). The high thermal stability of laser-glazed NARloy-Z is due to the short diffusion

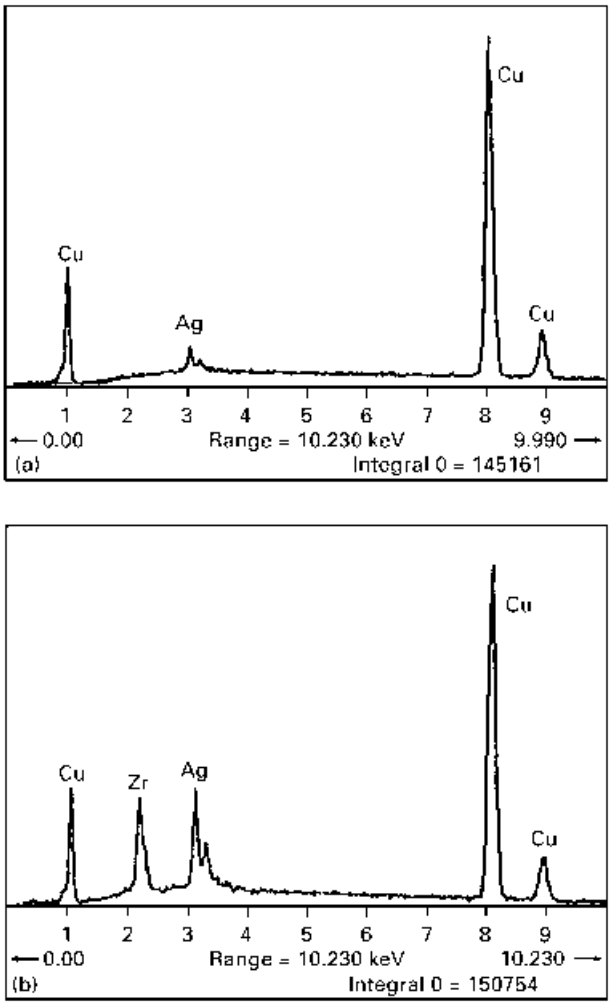

Figure 17 EDS spectrum of (a) matrix and (b) precipitate from Fig. 16.

distance of solute atoms (i.e. separation between precipitates is small). This feature also prevents precipitation at the grain boundaries. The laser-glazed and EB-processed alloys also underwent rapid melting and solidification, resulting in an extended solid solubility of Zr solute atoms into the Cu matrix.

In wrought NARloy-Z, Zr is introduced to suppress discontinuous precipitation and to absorb oxygen by forming Zr_2O_3. At high temperatures, Zr_2O_3 is believed to improve mechanical properties by preventing grain growth [5]. The wrought alloy contained Zr_2O_3 as well as Ag- and Zr-rich intermetallic phases. The actual microstructure consisted of relatively large grains with non-uniform distribution of intermetallic Zr- and Ag-rich phases (Fig. 5). These microstructural features contribute to lower mechanical properties at elevated temperatures $> 538\,^{\circ}C$ (1000°F). In particular, the large grain size lowers ductility [1].

Under equilibrium conditions, the maximum solid solubility of Zr is about 0.15 wt % in the Cu matrix at $\sim 822\,^{\circ}C$ (1512°F), decreasing as temperature decreases. NARloy-Z contains about 0.5 wt % Zr and the excess Zr precipitates either as Zr-rich intermetallic phase or as zirconium oxide. Inherent rapid melting and solidification that occurred in the laser and EB glazing processes, created a non-equilibrium condition thereby extending the solid solubility of Zr in the

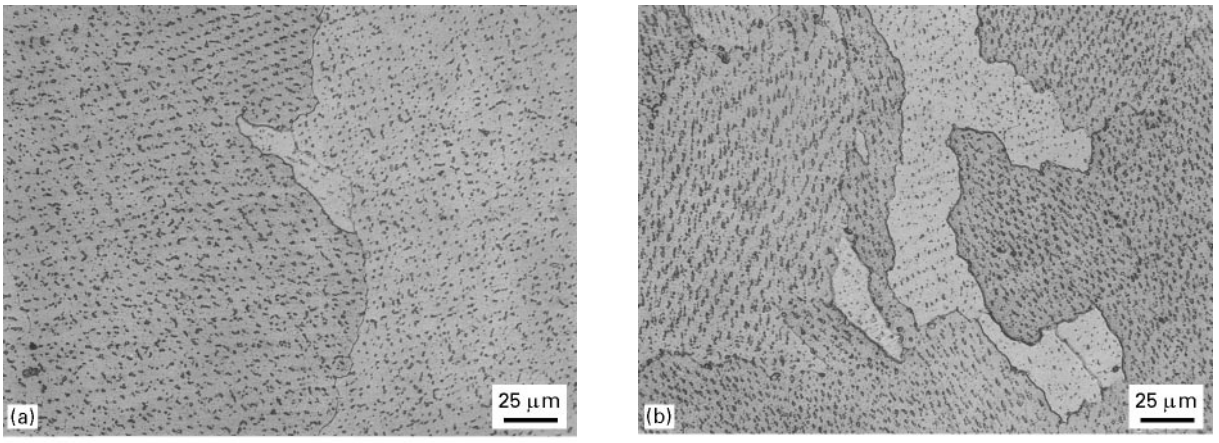

Figure 18 Laser-glazed NARloy-Z showing uniform distribution of second phases in Cu matrix after exposure at 760 °C (1400 °F) for (a) 24 and (b) 48 h.

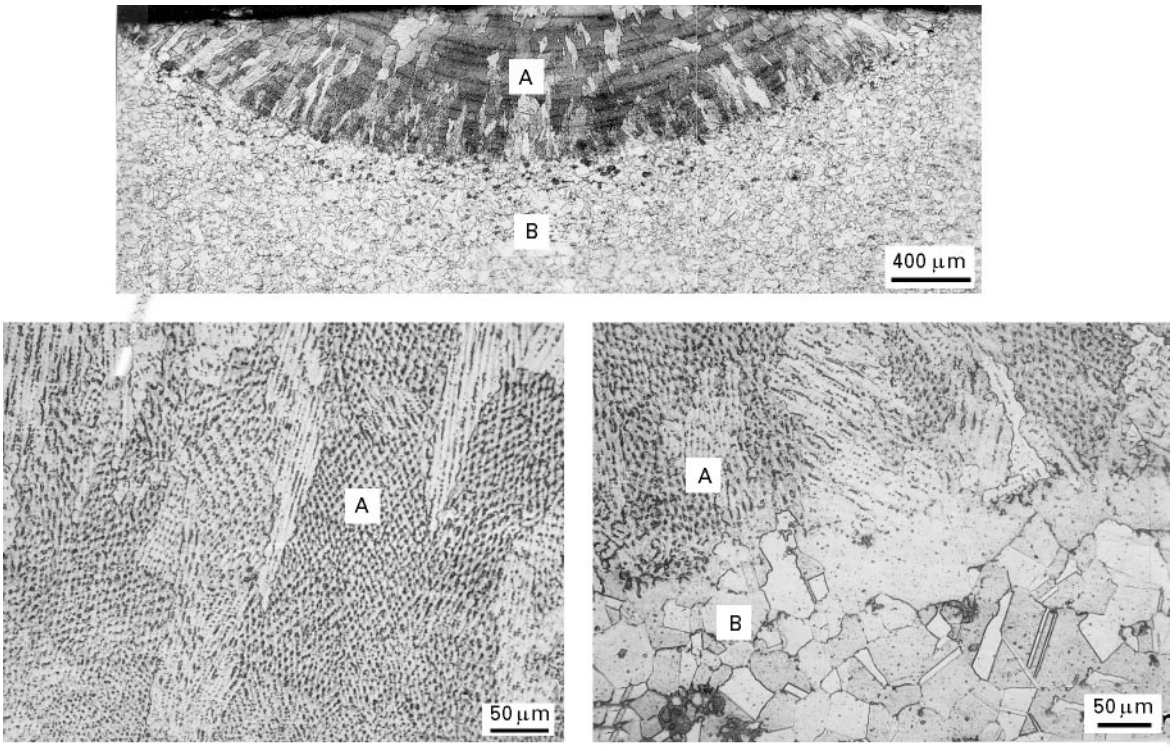

Figure 19 Electron beam-processed NARloy-Z with uniform distribution of second phases in Cu matrix at a melt depth of ~0.6 mm (25 mils).

copper matrix. The atomic size of Zr (0.162 nm) is larger (~30%) than the Cu matrix (0.1278 nm). Due to extended solid solubility of Zr atoms, the lattice strain was developed in the Cu matrix which probably changed the kinetics of Ag precipitation (compare Figs 6b and 14b). Ag precipitated as elemental Ag in laser-glazed NARloy-Z, whereas Ag- and Zr-rich intermetallic precipitates were observed in the wrought alloy (Fig. 9 and 15). The Ag and Zr alloying additions appear to play different roles in the wrought NARloy-Z versus the laser-glazed or EB-processed alloys, although all three forms retained the overall Cu–3% Ag–0.5% Zr composition.

In the laser and EB-processed alloys, Zr is present in the Cu matrix as solid solution and appears to stay in the matrix up to 760 °C (1400°F) and does not precipitate out. These factors probably contribute to their higher microstructural stability, higher hardness and enhanced thermal stability (Figs 1 to 3). Therefore, the EB or laser glazing approach can be used to enhance the life of SSME–MCC or other advanced MCC which use NARloy-Z as liner material.

4.4. Fractography

The fractured surface of the wrought alloy with the conventional heat treatment, tested at 538 °C, displayed dimpled features (Fig. 22a and b) which were characteristic of the ductility (60% elongation) in these specimens. A number of cracks were visible on

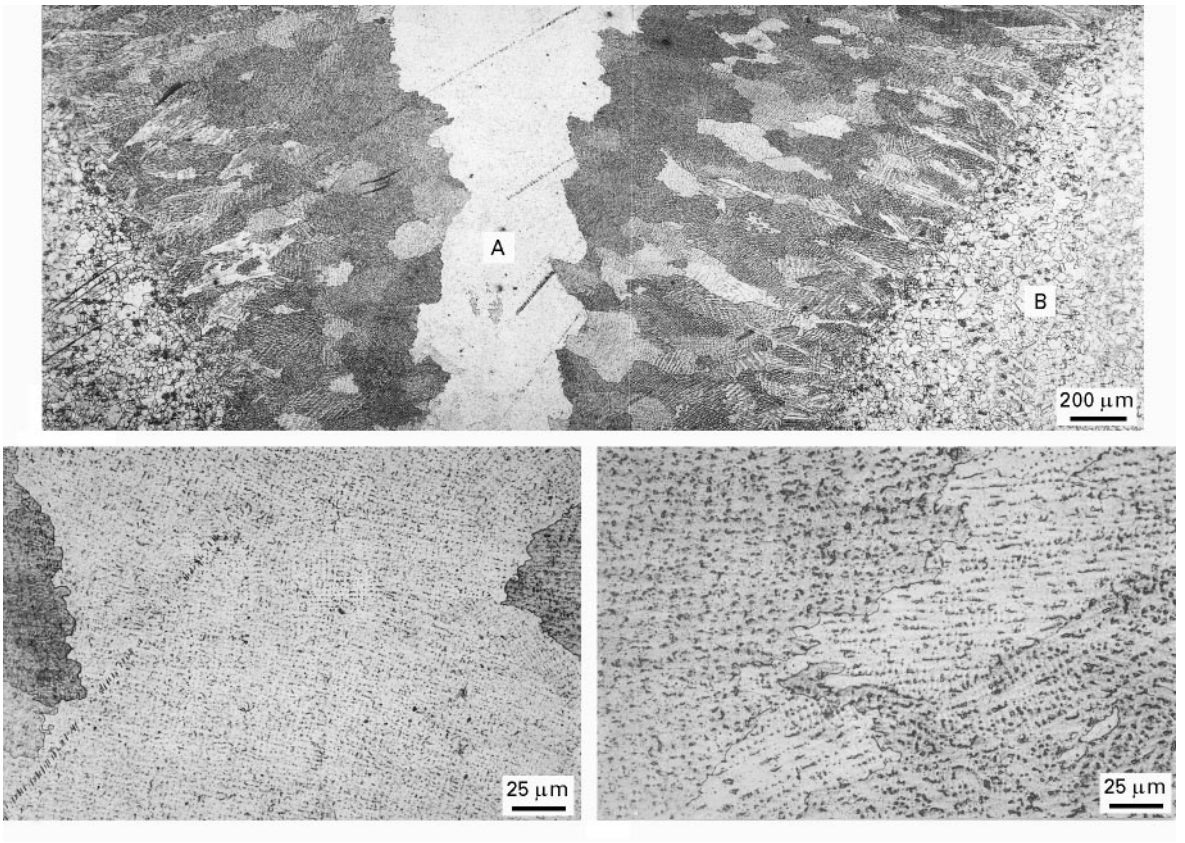

Figure 20 Electron beam-processed NARloy-Z showing uniform distribution of second phases in Cu matrix at melt depth of ~2 mm (80 mils).

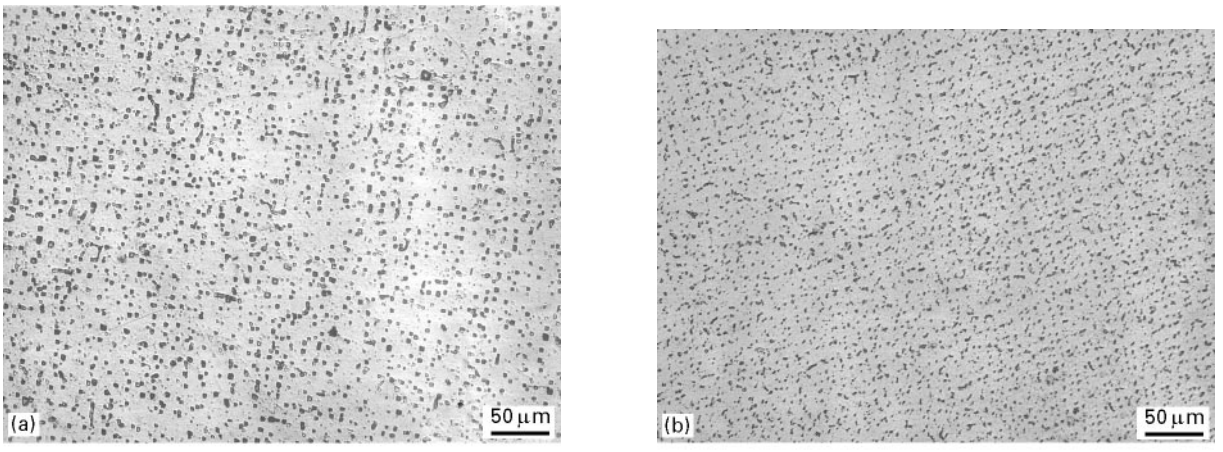

Figure 21 Electron beam-processed NARloy-Z showing uniform distribution of faceted second phases in Cu matrix after 24 h at (a) 705 °C (1300 °F) and (b) 760 °C (1400 °F).

the specimen surface (Fig. 22c and d) adjacent to the fracture surface. The electron beam glazed specimens also displayed dimpled fracture surfaces (Fig. 23a and b). The dimple size was more uniform for the glazed specimen in comparison to the non-glazed specimens (Figs 23a and 22b), consistent with the higher ductility of the glazed specimens. Similarly, the specimen surface adjacent to the fracture surface of the glazed specimens displayed more homogeneous deformation (Fig. 23c and d) and the non-glazed specimens (Fig. 22c and d). The homogeneous deformation and uniform dimple size distribution of the glazed specimens can be attributed to the extended solid solubility of Zr due to glazing and the consequent homogeneity of precipitation in the glazed microstructure (Figs 19–21). Fractographic features of the laser-glazed specimens were comparable to that of the electron beam glazed specimens, consistent with the similarity in tensile properties. Clearly, the microstructure is responsible for the superior tensile properties of glazed NARloy-Z. The fractographic features, consistent with the microstructure, confirm the observed advantages of glazing on tensile properties of wrought NARloy-Z.

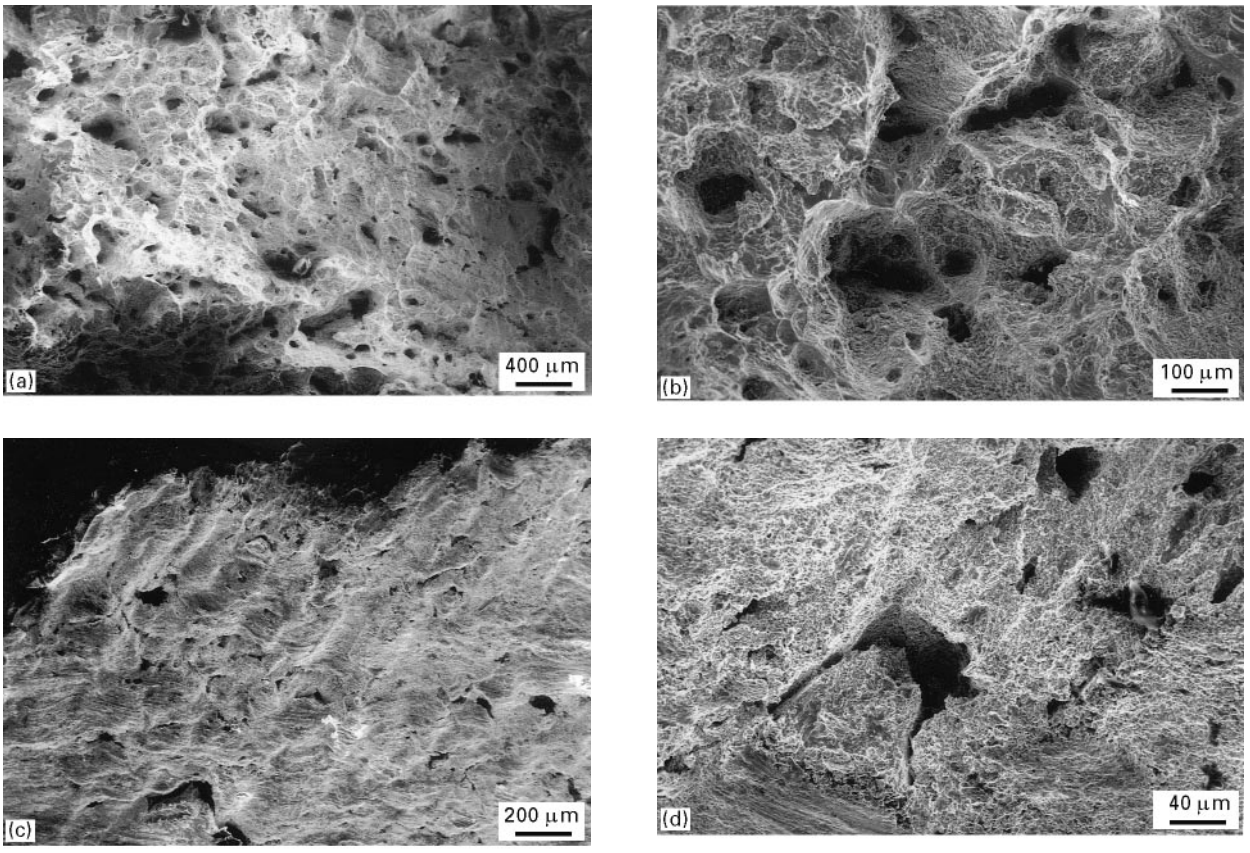

Figure 22 SEM fractograph of tensile specimen wrought NARloy-Z showing (a) low and (b) high magnification fractured surface; (c) and (d) high magnification surface adjacent to fracture.

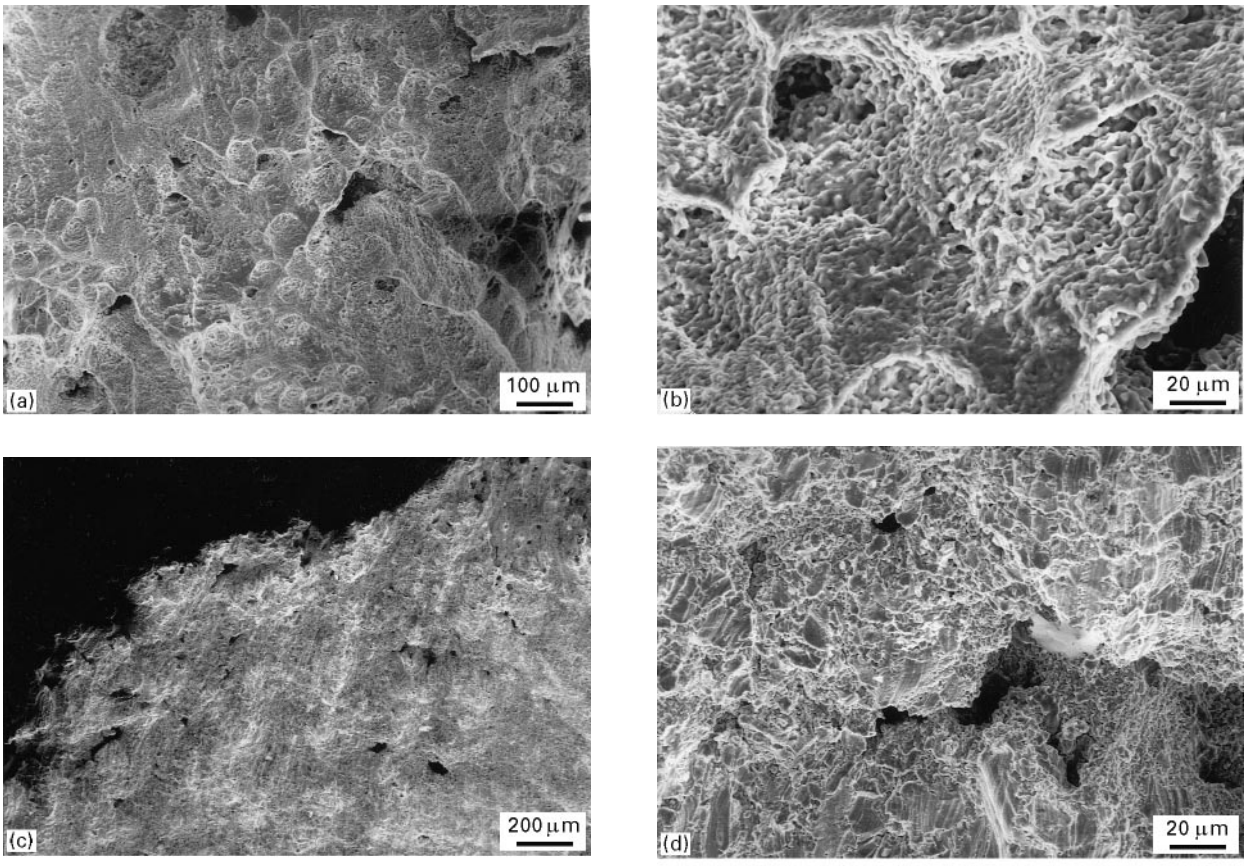

Figure 23 SEM fractograph tensile specimen (EB glazed + aged at 1400 °F (760 °C) for 2 h and He gas quenched) showing (a) low and (b) high magnification fractured surface: (c) and (d) high magnification specimen surface adjacent to fracture.

5. Summary

Microstructural evolution and precipitation morphology were investigated in wrought, laser-glazed, and electron beam-processed NARloy-Z samples by exposing them to temperatures from 593 to 760 °C (1100 to 1400°F). The results are summarized below and are applicable to NARloy-Z MCC liner.

5.1. Wrought alloy

1. Large grained microstructure (150 to 300 μm) had 15% lower hardness than the laser-glazed alloy.
2. Zr- and Ag-rich intermetallic phases were observed at grain boundaries and in the Cu matrix after exposure to temperatures above 593 °C (1100°F).
3. Non-uniform microstructure and precipitate free zones (PFZs) were formed after exposure to temperatures above 605 °C (1120°F).

5.2. Laser-glazed and electron beam-processed NARloy-Z

1. The hardness of laser- or EB-glazed NARloy-Z was approximately 15% higher than the wrought alloy and remained higher even after long exposures to elevated temperatures up to 760 °C (1400°F). The higher hardness was due to fine-grained microstructure (50–100 μm) with uniform distribution of second phase in the matrix.

2. Grain boundary precipitation and PFZ were not observed.

3. Extended solid solubility of Zr in the Cu matrix probably contributed to solid solution strengthening, which changed the Ag precipitation and coarsening kinetics to an aligned faceted morphology.

4. Microstructure was thermally stable up to 760 °C (1400°F).

5. Yield and ultimate tensile strengths of laser- and EB-glazed NARloy-Z were higher ($>20\%$) than the wrought alloy.

6. Ductility of glazed NARloy-Z can be increased by as much as 33% compared to the wrought alloy by giving suitable heat treatment while maintaining equivalent levels of strength.

References

1. P. S. CHEN and J. H. SANDERS, "An Investigation on the Ductility Loss of VPS NARloy-Z at Elevated Temperatures", (IIT Research Institute/MRF, 1992).
2. J. S. SINGH, G. JERMAN, R. POORMAN and B. N. BHAT, "Microstructural Evolution Of NARloy-Z At Elevated Temperatures" NASA Technical Memorandum No. 108419, Marshall Space Flight Center Huntsville, AC, 1993.
3. J. S. ANDRUS and R. G. BOURDEAU, "Thrust Chamber Material Technology Program", (Pratt & Whitney, West Palm Beach, FL, 1989).
4. D. B. MORGAN and A. C. KOBAYASHI, "Main Combustion Chamber and Cooling Technology", (Aerojet, Sacramento, CA, 1989).
5. J. S. SANDERS, "An Investigation of Main Combustion Chamber Liner 4011 Degradation", (IIT Research Institute/Metallurgy Research Facility (MRF), 1992).
6. N. E. PATON and W. M. ROBERTSON, "Metallurgy of NARloy-Z", (Rocketdyne, Canoga Port, CA, 1973).
7. J. S. SINGH, G. JERMAN, R. POORMAN and B. N. BHAT, "Microstructural stability of wrought, laser and electron beam glazed NARloy-Z at elevated temperatures", (NASA-Marshall Space Flight Center (MSFC) TM, 1993) no. 108431.

Received 17 March
and accepted 24 May 1995